High Frequency Modeling for Cable and Induction Motor Over-voltage Studies in Long Cable Drives

A. F. Moreira T. A. Lipo G. Venkataramanan
University of Wisconsin-Madison
Dept. of Electrical and Computer Engineering
1415 Engineering Dr., Madison, WI, USA, 53706

S. Bernet
ABB Corporate Research
Electrical Drive Systems (DECRC/E4)
Speyerer Strasse 4, Heidelberg, Germany, D-69115

***Abstract*-High frequency simulation models for power cables and motors are the key tools that aid a better understanding of the over-voltage problem in PWM drives with long feeders. In this paper, the frequency responses of the cable and the motor windings are obtained experimentally and suitable models are developed to match the experimental results. Several lumped segments incorporating a lossy representation of the line is used to model the cable. The cable and induction motor models may be implemented using a computational tool such as Matlab, thereby providing a convenient method to analyze the over-voltage phenomena. Simulation and experimental results are presented for a typical 3 hp induction motor, showing the suitability of the developed simulation models. The most promising dv/dt filter networks are also investigated through simulation analysis, and a design approach based on a trade off between filter losses and motor peak voltage is proposed. Experimental results of a RC Filter at the motor terminals demonstrate the validity of the simulation models.**

LIST OF SYMBOLS AND ABBREVIATIONS

R_s, L_s, R_{p1}, R_{p2}, C_{p1}, C_{p2}	Parameters of the high frequency model of the cable per unit length.
Z_{sc}, Z_{oc}	Cable short and open circuit impedances.
R_e, L_d, R_t, L_t, C_t, C_g, R_g	Parameters of the high frequency model of the motor per phase.
Z_{pn}, Z_{pg}	Phase-to-neutral and phase-to-ground motor impedances.
f_{low}, f_{high}	Lowest and highest test frequencies in the impedance measurements.
$f_{pole\text{-}Zpn}$	Frequency of the first pole in the frequency response of the phase-to-neutral motor impedance.
$f_{zero\text{-}Zpn}$	Frequency of the first zero in the frequency response of the phase-to-neutral motor impedance.

I. INTRODUCTION

Over-voltage problems in long cable drives, due to steep voltage pulse rise time, have become an important research area during the last decade. The over-voltage phenomenon is usually described using the traveling wave and reflection phenomena: a voltage pulse, initiated at the inverter, being reflected at the motor terminals due to a mismatch between the surge impedance of the motor and the cable. However, the magnitude of the over-voltage depends on the pulse rise time and on the characteristics and length of the cable [1,2,3,4]. The motivation for the work presented in this paper is the lack of good simulation approaches that can be used to accurately investigate the over-voltage phenomena. Therefore, the objective of this paper is to study the motor over-voltage phenomena in a definitive manner by developing accurate and fast simulation models for power cables and motors that allow a better understanding of the over-voltage problem. The models provide a convenient tool that can be utilized to benchmark the best dv/dt filter solution for a particular drive.

For the power cable, it is well known that distributed-parameter representation provides more accurate results in the study of high frequency transients than the lumped-parameter models [5]. However, lumped-parameter representation of the transmission line can be successfully used to analyze the over-voltage phenomena if adequate number of segments is used in the calculation [4]. In regard to the properties of the line, early papers have proposed the use of lossless characteristics [6,7,8], which leads to a considerable amount of inaccuracy. A recently proposed lossy line power cable representation yields more accurate results [4]. The use of a distortionless line representation was proposed in [9]. Preliminary investigations indicate it is still not sufficiently accurate to investigate the over-voltage problem, especially for very long cable drives. The inclusion of distortion has demonstrated to be important for an accurate analysis of the over-voltage. These issues are addressed in Section II, wherein a practical multiple segment lumped parameter model is proposed for modeling the power cable.

In Section III, high frequency representation for the induction motor is developed. Regarding the induction motor model, a simple R-L circuit has been used by most of the papers in the literature [6,7,8]. This model is definitely unable to capture all the high frequency content that is present in PWM voltage pulse. Some references have shown the necessity to have a different model for the induction motor other than the just a R-L circuit [4,9,10,11]. Among them, references [4,10,11] have successfully presented a high frequency induction motor model to calculate the over-voltage in long cable drives. In this paper, an improved motor model is also developed based on the model from [4,10,11], which gives better results in verifying the over-voltage phenomena in long cable drives.

The suggested high frequency models for power cables and motor are applied for specific case studies in the subsequent sections. These models are implemented to perform computer simulations using Matlab. The simulation program is very useful for the over-voltage analysis and provides a

convenient tool for a more reasonable design of the dv/dt filters. The most important dv/dt filter networks are investigated and design equations for each topology are presented. Through simulation and analysis, an alternative design is suggested based on the comparison between filter losses and motor terminal peak voltage. Experimental results of the over-voltage and of the application of the RC Filter are presented showing the validity of the simulation models.

II. High Frequency Model of the Power Cable

An adequate estimation of the power cable parameters is needed in order to have an accurate computation of the over-voltage. Previous authors have suggested to estimate the cable parameters by using equations related to the geometrical configuration of the cable. These approximations were found to be vastly different than actual parameter values because they do not include the frequency dependency in the calculation. Therefore, the cable parameters are estimated through experimental analysis by checking the frequency response of the power cable impedance. Fig. 1 shows a schematic of one of six possible active switch positions in a typical inverter fed motor drive. As can be seen, the connection between inverter and motor will have two phases in parallel and the other phase as returning cable. Therefore, it is suggested to measure the power cable impedance characteristics in this configuration. Two types of tests have been carried out: measurement of short circuit and open circuit impedances. The impedance measurements have been carried out for an unshielded four-wire cable (3 phases + 1 ground). The experiments were conducted using one-meter sample of the following cable gauges: #6, #8, #10, #12, and #14 AWG. The frequency dependent nature of the power cable parameters can be promptly verified from the frequency response plots. Figs. 2, 3, and 4 show the variation of the short circuit, open circuit, and surge impedances as a function of frequency for #6 AWG cable, respectively. Similar plots have been obtained for the other cable gauges. In these plots, the dots represent the frequency response obtained experimentally and the continuous line is the frequency response simulated in Matlab using the proposed high frequency model. Since the over-voltage phenomena must be evaluated over the frequency spectrum of the voltage pulse, it would be incorrect to assign a unique value for the cable parameters, which could be associated to the voltage pulse dominant high frequency [9]. Instead, the cable parameters can be estimated from a high frequency model for which the calculated frequency response matches the response obtained experimentally. Fig. 5 shows the suggested equivalent circuit for the cable that provide a sufficiently accurate frequency response for the short and open circuit measurements, and thus for the cable surge impedance. The parameters of the cable model are calculated from the short circuit impedance Z_{sc} and open circuit impedance Z_{oc} frequency responses using the following equations.

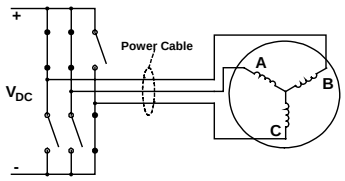

Fig.1: Schematic of one of six possible active switch positions in a drive. Phases A and B are in high potential and phase C is in low potential.

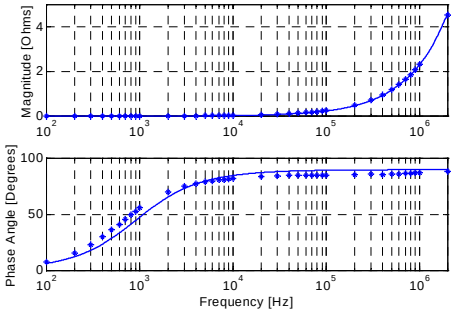

Fig. 2: Short circuit impedance frequency response. Solid line: simulation results. Stars: Experimental results.

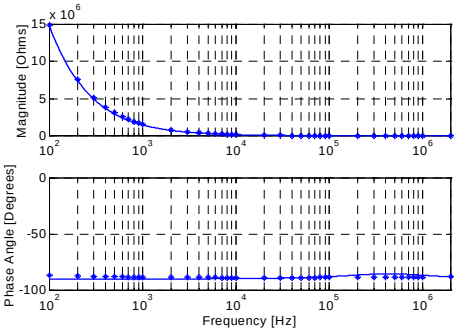

Fig. 3: Open circuit impedance frequency response. Solid line: simulation results. Stars: Experimental results.

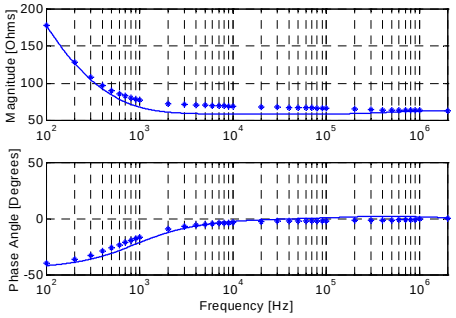

Fig. 4: Cable surge impedance frequency response. Solid line: simulation results. Stars: Experimental results.

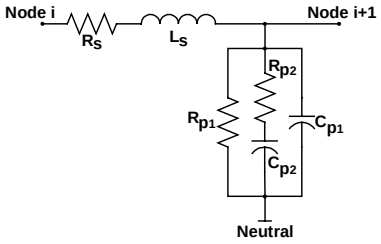

Fig.5: High frequency model of the power cable per unit length.

TABLE I
PARAMETERS OF THE HIGH FREQUENCY MODEL FOR VARIOUS CABLE GAUGES

Cable Gauge	R_s [mΩ]	L_s [μH]	R_{p1} [MΩ]	R_{p2} [kΩ]	C_{p1} [pF]	C_{p2} [pF]
6	1.5	0.24	173.9	13.9	137.1	22.5
8	6.0	0.20	262.1	21.2	119.7	15.3
10	7.0	0.28	221.7	18.9	125.4	17.7
12	7.5	0.26	218.8	22.8	104.7	16.8
14	16.0	0.29	265.7	25.4	93.9	16.8

$$R_s = \frac{2}{3} Real\{Z_{sc}\}_{f_{low}} \quad (1)$$

$$L_s = \frac{2}{3}\frac{1}{2\pi f_{high}} Imag\{Z_{sc}\}_{f_{high}} \quad (2)$$

$$R_{p1} = 2\left(Real\{Z_{oc}\}_{f_{low}}\right)\left[\left(\frac{Imag\{Z_{oc}\}_{f_{low}}}{Real\{Z_{oc}\}_{f_{low}}}\right)^2 + 1\right] \quad (3)$$

$$R_{p2} = 2\left(Real\{Z_{oc}\}_{f_{high}}\right)\left[\left(\frac{Imag\{Z_{oc}\}_{f_{high}}}{Real\{Z_{oc}\}_{f_{high}}}\right)^2 + 1\right] \quad (4)$$

$$C_{p2} = \left[\left(2\pi f_{high}\right)\left(\frac{Real\{Z_{oc}\}_{f_{high}}}{Imag\{Z_{oc}\}_{f_{high}}}\right) R_{p2}\right]^{-1} \quad (5)$$

$$C_{p1} = \left[\left(2\pi f_{low}\right)\left(\frac{Real\{Z_{oc}\}_{f_{low}}}{Imag\{Z_{oc}\}_{f_{low}}}\right) R_{p1}\right]^{-1} - C_{p2} \quad (6)$$

The frequency response calculated from the high frequency model is in a good agreement with the measured characteristics and the proposed lumped cable model may be used in the simulation analysis of the over-voltage. Table I summarizes the high frequency model parameters calculated for each cable gauge using the aforementioned equations.

III. HIGH FREQUENCY MODEL OF THE AC MACHINE

Another key factor for an accurate over-voltage analysis is the high frequency representation of the ac motor input impedance, which must be also valid over the frequency range of the voltage pulse. It is not necessary to verify how voltage distributes inside the ac machine winding in order to calculate the over-voltage. It is important, rather, to know the value of the ac motor input impedance and how it varies as a function of frequency. The proposed model for the ac motor input impedance is based on the high frequency model suggested in [10,11], which has been successfully used in calculating the over-voltage [4]. This section analyzes in detail the high frequency ac motor model with newly introduced modifications. The parameters of the model are derived using the frequency responses of the phase-to-neutral impedance Z_{pn} and phase-to-ground impedance Z_{pg}, as suggested in [10,11].

Figs. 6 and 7 show schematics of the experimental setup to measure the frequency responses of the phase-to-neutral and phase-to-ground impedances. The machines tested in laboratory are dual voltage ac induction motors. Dual voltage machines can commonly be connected in "delta" or "star" configuration, for a lower or a higher voltage, respectively.

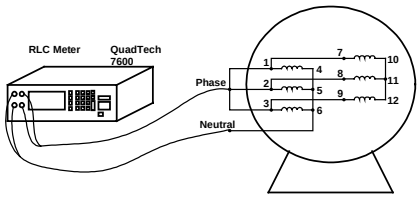

Fig. 6: Measurement of the phase-to-neutral impedance Z_{pn}.

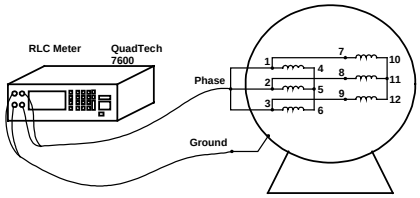

Fig. 7: Measurement of the phase-to-ground impedance Z_{pg}.

Usually some of the terminals of these machines are inaccessible, such as the terminals numbered 10, 11 and 12 in Figs. 6 and 7. Therefore, the following procedures are taken:

- Since terminals 10, 11 and 12 are not accessible, the phase-to-neutral and phase-to-ground impedances are measured for the machine connected in delta configuration;
- Since the internal neutral (terminals 10-11-12) is not accessible, the phase-to-neutral impedance is measured between terminals 1-2-3 (phase) and terminals 4-5-6 (external neutral). The measured values are thus divided by 2, in order to account for the other parallel set of windings (7-10, 8-11, and 9-12).

Fig. 8 shows the proposed per-phase high frequency motor model that is used in the calculation of the over-voltage analysis. The suggested model is a lumped-parameter representation of the motor input impedance for which the calculated frequency response matches the experimental response. The dynamic d-q model is partly responsible for capturing the low frequency transients, while the remaining R-L-C network is responsible to represent the high frequency phenomena. Winding-to-ground capacitance and winding turn-to-turn capacitance play the major role in the high frequency phenomena. Their relation with the leakage inductance forms the dominant poles in the frequency response. The parameter C_g represents the winding-to-ground capacitance. The parameter R_g is added in the circuit to represent the dissipative effects that are present in the motor frame resistance. The circuit formed by the parameters R_t, L_t, and C_t is the part of the network responsible to capture the second resonance in the frequency response, which is related to the winding turn-to-turn capacitance. The parameter R_e is responsible to account for the losses introduced by eddy current inside the magnetic core. In order to estimate the parameters of the high frequency part of the model it is suggested to replace the d-q model by a lumped-inductance L_d, which represents the leakage inductance of the machine winding. The high frequency model proposed in Fig. 8 has been evaluated for various induction motor ratings. The behavior of the phase-to-neutral, phase-to-ground and

motor input impedances as a function of frequency for a typical random wound 3 hp induction motor are shown in Figs. 9, 10, and 11, respectively. From the frequency responses obtained experimentally, the parameters of the high frequency model can be calculated using the following expressions.

$$C_g \approx \frac{1}{2}\left(\frac{1}{3}\right)\frac{1}{(2\pi f_{low})\, Mag\{Z_{pg}\}_{f_{low}}} \quad (7)$$

$$R_g \approx 3 \times Real\{Z_{pg}\}_{f_{high}} \quad (8)$$

$$L_d \approx \frac{2}{C_g}\left(\frac{1}{2\pi f_{pole\text{-}Z_{pn}}}\right)^2 \quad (9)$$

$$R_e \approx 3 \times Mag\{Z_{pn}\}_{f_{pole\text{-}Zpn}} \quad (10)$$

$$C_t \approx \frac{C_g}{10} \quad (11)$$

$$L_t \approx \frac{1}{C_t}\left(\frac{1}{2\pi f_{zero\text{-}Z_{pn}}}\right)^2 \quad (12)$$

$$R_t \approx 3 \times Real\{Z_{pn}\}_{f_{zero\text{-}Zpn}} \quad (13)$$

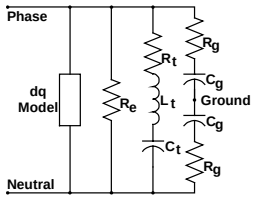

Fig. 8: Per-phase representation of the AC motor including the high frequency model and the dynamic dq model.

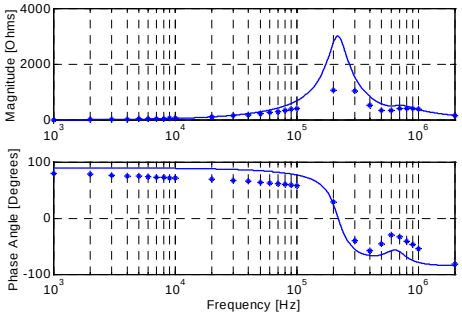

Fig. 9: Phase-to-neutral impedance frequency response. Solid line: simulation results. Stars: Experimental results.

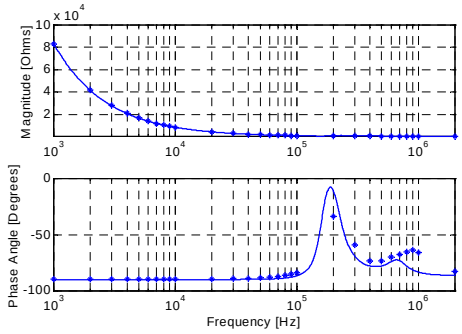

Fig. 10: Phase-to-ground impedance frequency response. Solid line: simulation results. Stars: Experimental results.

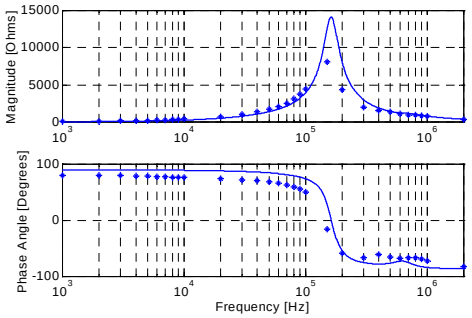

Fig. 11: Motor input impedance frequency response. Solid line: simulation results. Stars: Experimental results.

TABLE II
PARAMETERS OF THE HIGH FREQUENCY MOTOR MODEL FOR VARIOUS RATINGS

Ratings [hp]	C_g [pF]	R_g [Ω]	L_d [mH]	R_e [kΩ]	C_t [pF]	L_t [mH]	R_t [kΩ]
2	290	15.3	5.1	3.9	29	0.27	0.324
3	314	35.5	4.0	5.6	31.4	2.7	1.15
7.5	700	36.2	0.55	3.3	70	0.21	0.94
10	704	23.2	1.3	1.4	70.4	0.09	0.086
15	1810	0.2	0.53	0.7	181	0.0014	—
25	1550	22.9	0.41	1.03	155	0.0016	—
40	260	12	0.86	2.5	26.1	0.48	0.1

The calculated frequency response using the proposed high frequency model has shown to be in a good agreement with the experimental results. Therefore, the proposed approach may be used to represent the motor input impedance in the over-voltage simulation analysis. Table II summarizes the parameters of the high frequency model for various hp ratings of induction motor.

IV. SIMULATION AND EXPERIMENTAL ANALYSIS OF THE OVER-VOLTAGE

A flexible program was built in Matlab that allows one to evaluate the over-voltage problem accurately for different cable lengths and for different voltage pulse rise times. In the program one chooses the number of lumped sections as well as the simulation time step. The whole system can be simulated in a two axes (d-q) approach, which reduces the number of differential equations. The numerical integration is realized using Runge-Kutta Method order 4 [4]. Simulation results were obtained for a system with a 3 hp motor and #6 AWG driving cable with different lengths. Experimental results were also obtained to validate the simulation study. Figs. 12 to 14 shows the over-voltage waveforms for different power cable lengths. In each figure, the left side plots are the simulation realized in Matlab using the aforementioned high frequency models and the right side plots are the experimental waveforms. The accuracy of the simulation models in predicting the over-voltage is readily evident from the plots. Additional simulation and experimental results are shown in Figs. 15 and 16, where the behavior of the line-to-line voltage in the machine terminals can be examined as a function of the voltage pulse rise times for 20 m and 70 m cable length, respectively. It can be

concluded from these results that the proposed over-voltage simulation approach is a very useful tool to predict with reasonable accuracy the magnitude of the over-voltage in the machine winding. These models are used to evaluate the performance of various filter networks in the following section.

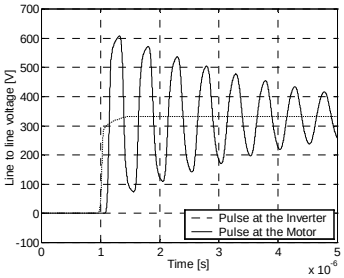

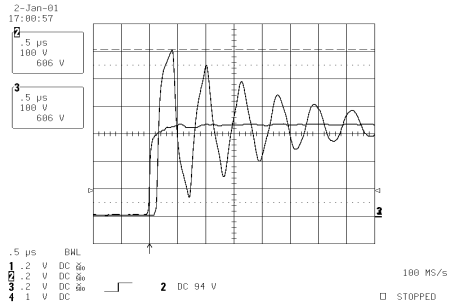

Fig. 12: Over-voltage waveforms. 3 hp induction motor. 20 meters cable length. Left plot: simulation. Right plot: experimental.

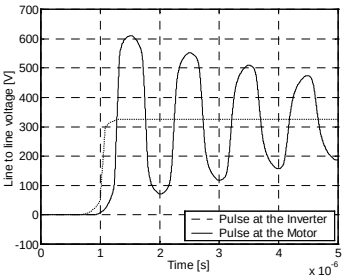

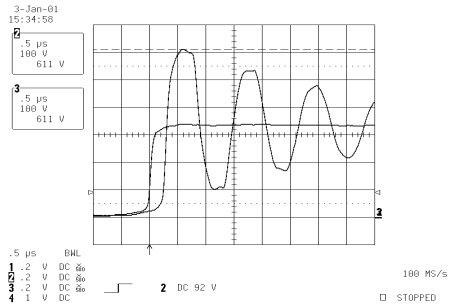

Fig. 13: Over-voltage waveforms. 3 hp induction motor. 40 meters cable length. Left plot: simulation. Right plot: experimental.

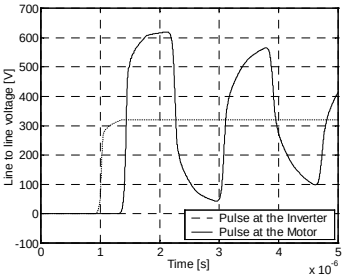

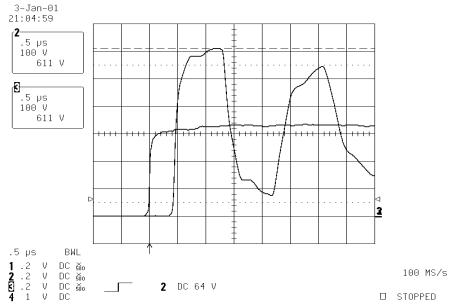

Fig. 14: Over-voltage waveforms. 3 hp induction motor. 70 meters cable length. Left plot: simulation. Right plot: experimental.

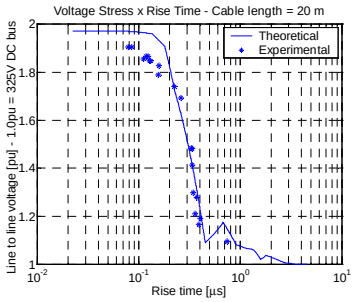

Fig. 15: Line-to-line voltage peak in pu versus rise time. 3 hp induction motor. 20 meters cable length. Solid line: simulation. Stars: experimental.

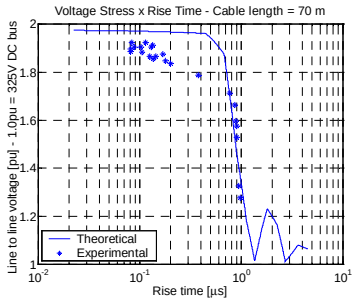

Fig. 16: Line-to-line voltage peak in pu versus rise time. 3 hp induction motor. 70 meters cable length. Solid line: simulation. Stars: experimental.

V. Modeling and Design of Filter Networks

Several filtering techniques have been proposed to mitigate the over-voltage problem in long cable PWM drives [6,7,8,12]. In general, these techniques include matching the cable surge impedance to the motor input impedance and increasing the voltage pulse rise time initiated at the inverter. The most relevant filter networks are found to be: RC and RLC filters at the motor terminals [6,7,12], RLC and LC+Clamping filters at the inverter output [7,8]. Table III

presents a summary of the configuration and design equations of these approaches. These equations are not sufficient to provide a suitable design for the filter topologies if one is looking for lower filter losses and lower peak voltage at the motor terminals. In reality, a closed form expression that gives the voltage peak in the motor terminal as a function of the filter parameters is too complex to be useful for design purposes. An alternative approach for the filter design could be based on simulation analysis rather than a closed form expression. It is suggested here to utilize the over-voltage simulation program developed in Matlab to find more suitable values for the filter topologies parameters. To realize this, simulation charts can be derived for each filter showing peak voltage and losses as function of the key parameters of the filter approaches. When pertinent, the concepts behind the filtering techniques may be used together with the simulation analysis in order to derive the most suitable design. Such design procedure for the RC filter is presented further.

The first step is to verify the matching characteristics between cable surge impedance and motor input impedance, since this is the starting point of the doubling effects. Fig. 17 shows the frequency dependence of these impedances. It can be observed for frequencies above tens of kilohertz that the impedances do not match it all. It is not adequate to analyze the impedance matching for unique value of impedances for a particular frequency. Rather, the analysis must be carried out for a broad range of frequencies, which would include the frequency responses of the cable and the motor impedances. The suggested design practice is to make the filter resistance equal to the cable surge impedance since the motor input impedance is much bigger than the cable surge impedance. But, the key issue is the choice of frequency at which the filter resistance should be made equal to the surge cable impedance. In the technical literature the impedance matching is usually analyzed at low frequencies around 100 to 200 Hz. This is not a good choice because the over-voltage problem appears for high frequencies above tens of kilohertz. Therefore, it is proposed to match the filter resistance to the value of the surge cable impedance for very high frequencies as shown in (14) for a star connection of the filter, where L_s and C_{p1} are parameters of the high frequency cable model.

$$R_{filter} = |Z_{surge\text{-}cable}|_{f\to\infty} \approx \sqrt{\frac{L_s}{C_{p1}}} \approx 42\,\Omega \qquad (14)$$

Fig. 18 shows the simulation results of the voltage reflection coefficient at motor terminals for three values of filter resistance, while the capacitance was fixed at C_{filter}=0.075μF. It can be observed that the best option is the value established in (14), which gives the closest to a zero magnitude for the voltage reflection coefficient, and thus the lowest peak over-voltage.

In the case of the filter capacitor, the objective is, through several simulation results, to choose a capacitor value for which the filter has lower losses and the motor experiences the lower line-to-line peak voltage. Fig. 19 shows the simulation results for several values of filter capacitance. The choice of the filter capacitor turns to be a trade-off between filter losses and peak voltage at the machine terminals. As the capacitance becomes large, the line-to-line peak voltage becomes lower and the filter losses become higher. Therefore, one can decide on the maximum allowable filter losses and then choose the filter capacitance to obtain the desired peak voltage at the motor terminals.

TABLE III
DESIGN EQUATIONS OF THE MOST SUITABLE FILTER NETWORKS

RC Filter at the Motor Terminals	RLC Filter at the Motor Terminals	RLC Filter at the Inverter Output	LC+Clamping Filter at the Inverter Output
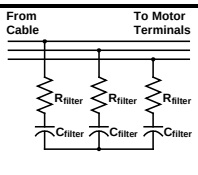	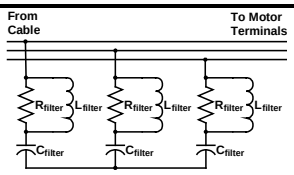	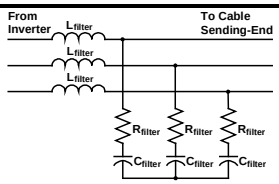	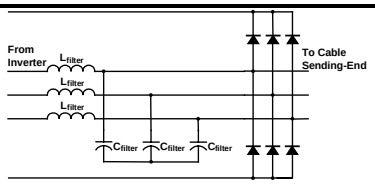
RC Filter at the motor terminals [6,12]	$R_{filter} = \lvert Z_{surge\text{-}cable}\rvert$ (15)	$C_{filter} = \dfrac{\tau_{rise}}{0.1054\,R_{filter}}$ (16)	
RLC Filter at the motor terminals [6]	$R_{filter} = \lvert Z_{surge\text{-}cable}\rvert$ (17)	$\exp(-\omega_n\tau_{rise})(1-\omega_n\tau_{rise}) = 0.9 \quad \dfrac{1}{R_{filter}C_{filter}} = 2\omega_n \quad \omega_n^2 = \dfrac{1}{L_{filter}C_{filter}}$ (18)	
RLC Filter at the inverter output [7]	$R_{filter} = \dfrac{\lvert Z_{surge\text{-}cable}\rvert}{2}$ (19)	$\exp(-\omega_n\tau_{rise})(1+\omega_n\tau_{rise}) = 0.9 \quad 2\omega_n = \dfrac{2L_{filter} + \lvert Z_{surge\text{-}cable}\rvert R_{filter}C_{filter}}{L_{filter}C_{filter}(2R_{filter} + \lvert Z_{surge\text{-}cable}\rvert)}$ (20) $\omega_n^2 = \dfrac{\lvert Z_{surge\text{-}cable}\rvert}{L_{filter}C_{filter}(2R_{filter} + \lvert Z_{surge\text{-}cable}\rvert)}$	
LC+Clamping Filter at the inverter output [8]	—	$0.3 \le \zeta \le 0.8 \quad \omega_n = \dfrac{2.16\zeta + 0.6}{\tau_{desired}} \quad \zeta\omega_n = \dfrac{1}{\lvert Z_{surge\text{-}cable}\rvert C_{filter}} \quad \omega_n^2 = \dfrac{1}{L_{filter}C_{filter}}$ (21)	

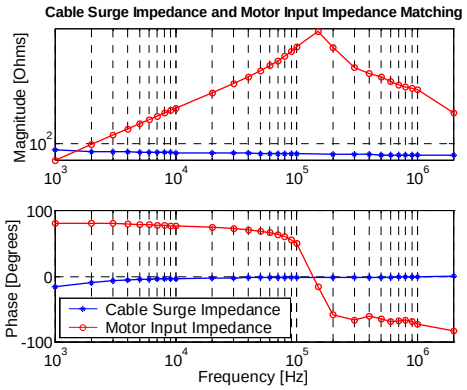

Fig. 17: Matching characteristics between cable surge impedance and motor input impedance as a function of frequency. Cable: #6 AWG. Motor: 3 hp.

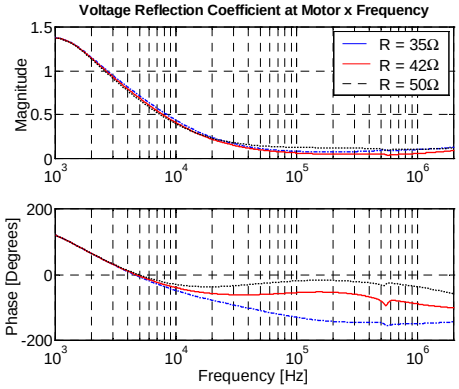

Fig. 18: Voltage reflection coefficient at the motor terminals as a function of frequency for various filter resistors. Cable: #6 AWG. Motor: 3 hp.

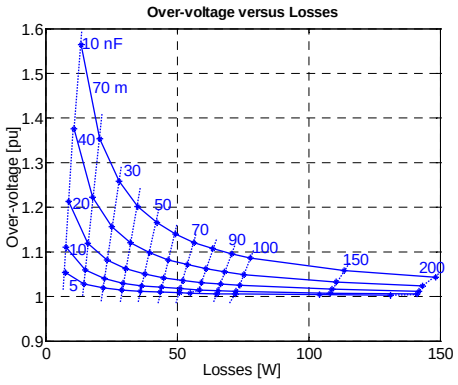

Fig. 19: Over-voltage versus filter losses (at 5 kHz) for various numbers of filter capacitors (in star connection) and for various cable lengths. Motor: 3 hp. R_f = 42 Ω. Voltage pulse rise time ≈ 100 ns.

It can be also verified from Fig. 19 that the filter capacitor choice to obtain the same level of line-to-line voltage is not unique independent of cable length, as commonly expected in the literature for the filter networks placed at the motor terminals. In this case, the total inductance of the line must be considered during the filter capacitor design. Thus, it can be concluded that the chart proposed by Fig. 19 is indeed very useful on the filter network design.

Several simulation and experimental analyses have been realized using the RC Filter at the motor terminals. Selected results are presented here. Fig. 20 shows simulation and experimental results for the 70 m cable length case using R_{filter} = 126 Ω and C_{filter} = 10 nF (filter in delta connection). These plots show the characteristics of the line-to-line voltage and the current through one of the RC filter branches. The correlation between simulation and experimental results can be promptly verified, showing the usefulness of the simulation program in studying the over-voltage problem and in the design of filter networks.

One important missing detail that should be mentioned here is related to the initial charge conditions across the various energy storage elements in the lumped-parameter segments of the cable during the simulation. At this point, it has not been possible to initialize the charge conditions of the cable in the proposed simulation program. It is however true that the current level in the machine for which the switching transient occurs will produce different amplitudes of over-voltage in the machine terminals. Figs. 21 and 22 shows experimental results demonstrating this fact. It can be observed that for higher current amplitudes, the line-to-line voltage is also higher. Incorporation of these issues is the subject of ongoing investigations and the results will be published in the future.

VI. Conclusions

This paper has proposed a Matlab based program intend to the analysis of the over-voltage phenomena in long cable PWM drives. The following are the main characteristics of the simulation program:

- The voltage pulse initiated at the inverter can be easily adjusted to better represent the reality. This is an important feature, since the characteristics of the over-voltage are strongly dependent on the harmonic contents of the voltage pulse.
- The power cable is represented as a transmission line with lossy characteristics and modeled using several lumped-parameter segments. The inclusion of distortion is very important to obtain a close representation of the over-voltage.
- A model for the motor input impedance intended for high frequency analysis has been also used. A high frequency motor model is very important to capture the high frequency transients.

The parameters of the cable and motor models have been derived from frequency response analysis of the cable and motor characteristic impedances, respectively, and a better representation of the cable-motor system is achieved intend to the over-voltage analysis.

Several simulation and experimental results have been presented showing the usefulness of the simulation program on the analysis of the over-voltage. Over-voltage charts as a function of the voltage pulse rise time and cable length were generated that allows one to accurately predict the voltage stress for various situations.

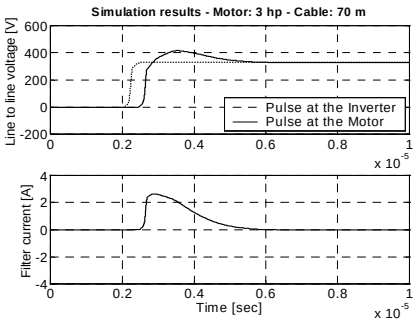

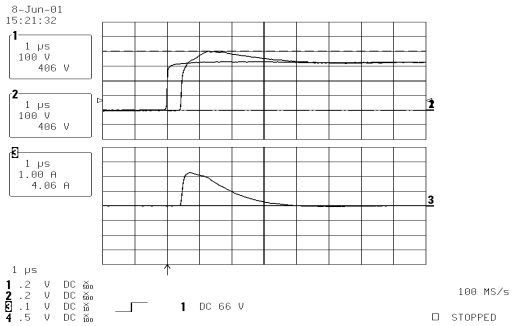

Fig. 20: Simulation (left plot) and experimental (right plot) results of the RC filter at the motor terminals. Motor: 3 hp. Cable length: 70 m. RC Filter: R_f = 126 Ω and C_f = 10 nF (delta connection). Voltage pulse rise time ≈ 100 ns.

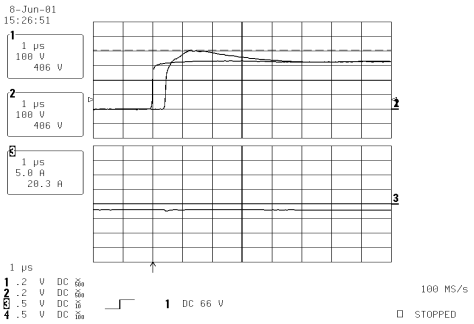

Fig. 21: Experimental results of the line-to-line voltage at low motor current level. Motor: 3 hp. Cable length: 70 m. RC Filter: R_f = 126 Ω and C_f = 10 nF (delta connection). Voltage pulse rise time ≈ 100 ns.

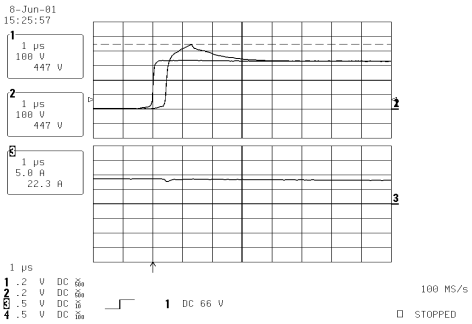

Fig. 22: Experimental results of the line-to-line voltage at high motor current level. Motor: 3 hp. Cable length: 70 m. RC Filter: R_f = 126 Ω and C_f = 10 nF (delta connection). Voltage pulse rise time ≈ 100 ns.

Design equations of the most relevant filter networks have been presented. Using the simulation program, a more thorough design approach has been proposed examining the RC filter at the motor terminals. Using this approach, the filter resistance is chosen according to the matching between cable surge and motor input impedances in the frequency domain. In addition, the filter capacitor is selected according to the desired voltage stress and filter losses. The proposed simulation model can be used in the design of the other filter networks as well.

ACKNOWLEDGMENT

This research work has been supported by the following entities: ABB Corporate R&D/Germany, WEMPEC at UW-Madison/USA, and UFMG and CAPES/Brazil.

REFERENCES

[1] E. Persson, "Transient Effects in Applications of PWM Inverters to Induction Motors," *IEEE Transactions on Industry Applications*, vol. 28, no. 5, pp. 1095-1101, Sep/Oct 1992.

[2] A.H. Bonnett "Analysis of the Impact of Pulse-Width Modulated Inverter Voltage Waveforms on AC Induction Motors," *IEEE Transactions on Industry Applications*, vol. 32, no. 2, pp. 386-392, Mar/Apr 1996.

[3] R. Kerkman, D. Leggate, and G. Skibinski, "Interaction of Drive Modulation & Cable Parameters on AC Motor Transients," *Proceedings of 31st IEEE Industry Applications Society Conference (IAS'96)*, vol. 1, pp. 143-152, San Diego, CA, USA, 1996.

[4] A. F. Moreira, T. A. Lipo, G. Venkataramanan, and S. Bernet, "Modeling and Evaluation of dv/dt Filters for AC Drives with High Switching Speed," to be published in the *Proceedings of 9th European Conference on Power Electronics and Applications (EPE'01)*, Aug. 27-29, Graz, Austria, 2001.

[5] P.C. Krause and K. Carlsen, "Analysis and Hybrid Computer Simulation of Multiconductor Transmission Systems," *IEEE Transactions on Power Apparatus and Systems*, vol. 91, pp. 465-477, Mar/Apr 1972.

[6] A. von Jouanne, D. Rendusara, and P.N. Enjeti, "Filtering Techniques to Minimize the Effect of Long Motor Leads on PWM Inverter-Fed AC Motor Drive Systems," *IEEE Transactions on Industry Applications*, vol. 32, no. 4, pp. 919-926, July/Aug. 1996.

[7] A. von Jouanne and P.N. Enjeti, "Design Considerations for an Inverter Output Filter to Mitigate the Effects of Long Motor Leads in ASD Applications," *IEEE Transactions on Industry Applications*, vol. 33, no. 5, pp. 1138-1145, Sep/Oct 1997.

[8] S.J. Kim and S.K. Sul, "A Novel Filter Design for Suppression of High Voltage Gradient in Voltage-Fed PWM Inverter," *Proceedings of 12th IEEE Annual Applied Power Electronics Conference and Exposition (APEC'97)*, vol. 1, pp. 122-127, Feb. 23-27, Atlanta, GA, USA, 1997.

[9] G. Skibinski, R. Kerkman, D. Leggate, J. Pankau, and D. Schlegel, "Reflected Wave Modeling Techniques for PWM AC Motor Drives," *Proceedings of 13th IEEE Annual Applied Power Electronics Conference and Exposition (APEC'98)*, vol. 2, pp. 1021-1029, Feb. 15-19, Anaheim, CA, USA, 1998.

[10] G. Grandi, D. Casadei, and A. Massarini, "High Frequency Lumped-parameter Model for AC Motor Windings," *Proceedings of 7th European Conference on Power Electronics and Applications (EPE'97)*, vol. 2, pp. 578-583, Trondheim, Belgium, 1997.

[11] A. Boglietti and E. Carpaneto, "Induction Motor High Frequency Model," *Proceedings of 34th IEEE Industry Applications Society Conference (IAS'99)*, Oct. 3-7, Phoenix, AR, 1999.

[12] G. Skibinski, "Design Methodology of a Cable Terminator to Reduce Reflected Voltage on AC Motors," *Proceedings of 31st IEEE Industry Applications Society Conference (IAS'96)*, San Diego, CA, USA, 1996.